ChemComm

Accepted Manuscript

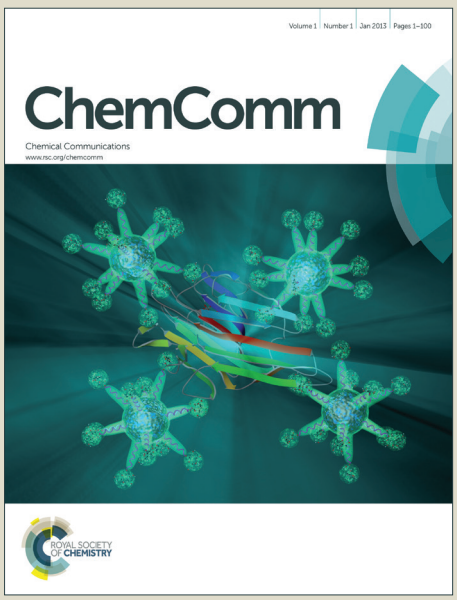

ROYAL SOCIETY OF CHEMISTRY

www.rsc.org/chemcomm

Journal Name

RSCPublishing

COMMUNICATION

Hyaluronic acid-polypyrrole nanoparticles as pH-responsive theranostics

Cite this: DOI: 10.1039/x0xx00000x

Dongjin Park[a], Youngnam Cho[b], Sung-Ho Goh*[c] and Yongdoo Choi*[a]

Received 00th January 2012,
Accepted 00th January 2012

DOI: 10.1039/x0xx00000x

www.rsc.org/

Doxorubicin-loaded hyaluronic acid-polypyrrole nanoparticles were developed for pH-responsive activatable fluorescence imaging and therapy of proliferating macrophages.

Atherosclerosis is the major reason for cardiovascular disease, which accounts for 39% of all global deaths under the age of 70.[1] Macrophages, representing up to 20% of the cells within atherosclerotic lesions, play a pivotal role both in the development of atherosclerosis, and also in atheroma plaque destabilization and rupture, an occurrence that frequently leads to thrombo-occlusive complications (*i.e.*, myocardial infarction and strokes).[2] Thus, antimacrophage therapeutic strategies including systemic modulation of macrophage activity and local photodynamic therapy using conventional and smart photosensitizers have been attempted.[3-5]

It has recently been reported that the majority of macrophages in atherosclerotic lesions are derived from local macrophage proliferation rather than the inflammatory monocyte recruitment from peripheral blood.[6] These reports reveal that targeting macrophage proliferation could be a new strategy to treat established atherosclerosis. However, few studies have evaluated antiproliferating agents.[6b,7] Here, we developed drug-loaded hyaluronic acid-polypyrrole nanoparticles (HA-PPyNP) as a smart theranostic platform for noninvasive fluorescence imaging and therapy of proliferating macrophages in atherosclerotic lesions (Fig. 1).

We first synthesized hyaluronic acid-conjugated polypyrrole nanoparticles (HA-PPyNP), and then antiproliferating agent doxorubicin (DOX) was loaded on the surface of HA-PPyNP by forming a charge complex between the highly negatively charged HAs and positively charged DOXs. Polypyrrole nanoparticles (PPyNP) are reported to have an immense absorption coefficient (*i.e.*, 10^4-fold to 10^6-fold higher than conventional organic fluorochromes) with a broad peak,[8] and therefore may have a great potential as ultra-efficient energy quenchers. We hypothesized that, when DOXs are located near a PPyNP surface, energy transfer from DOX to PPyNP is effective, resulting in the quenching of DOX fluorescence (OFF). Since the carboxylic acids of HA are negatively charged at an extracellular pH of 7.4, the charge complex between DOX and HA-PPyNP is relatively stable and fluorescence of DOX-loaded in HA-PPyNP (*i.e.*, DOX@HA-PPyNP) remains turned off while circulating in the blood stream. However, preferential accumulation of DOX@PPyNP into atherosclerotic plaques with leaky vascular structure and enhanced permeability,[9] followed by endocytosis by macrophage cells results in fluorescence activation of DOX; DOX release from HA-PPyNPs is stimulated by the loss of the negative charges of HA under acidic lysosomal conditions for pH < 5. Therefore, in contrast to free DOX, for which fluorescence is always turned on, and with unfavorable pharmacokinetic behavior, pH-responsive theranostic nanomedicine DOX@HA-PPyNP may have utility in fluorescence imaging with high target-to-background ratios and may be important for the treatment of proliferating macrophages with reduced systemic toxicity.

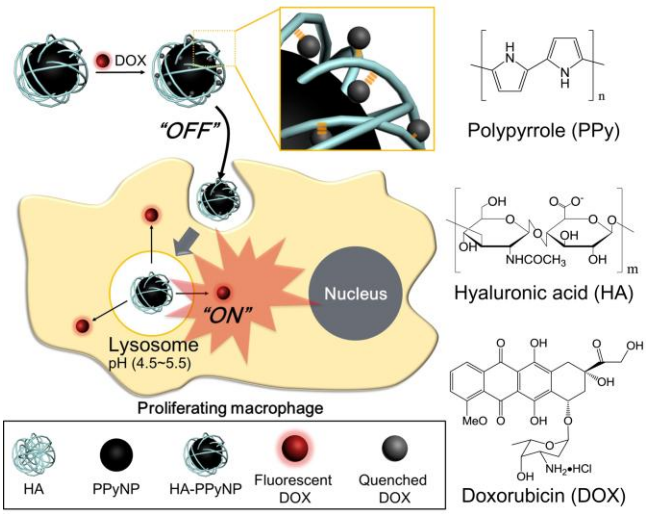

Fig. 1. Schematic diagram of the pH-responsive theranostic system. DOX forms a charge complex with HA on the surface of polypyrrole nanoparticles, leading to fluorescence quenching of DOX (OFF) through a FRET mechanism. When DOX-loaded HA-PPyNPs are taken up into the proliferating macrophage cells, DOX release from the PPyNP surface is stimulated, resulting in both the turn on of DOX fluorescence and therapy of the proliferating macrophages.

HA-conjugated PPyNP (HA-PPyNP) was prepared by adding HA polymers during PPyNP synthesis. HA with negatively charged carboxyl groups was expected to form physical crosslinking with the

positively charged polypyrroles via a charge-charge interaction; therefore, HA molecules could be incorporated on the surface of PPyNP during nanoparticle synthesis. The morphology of the prepared HA-PPyNP was round-shaped under scanning electron microscopy (Fig. S1a, ESI†). The mean hydrodynamic size and zeta potential of HA-PPyNP in an aqueous solution were 88.4 nm and −26.1 mV, respectively (Fig. S1c, ESI†). Since PPyNP prepared in the absence of HA has positive zeta potential (+5.47 mV), the negative zeta potential of HA-PPyNP indicates coverage of HA molecules on the surface of PPyNP. The FT-IR spectra of HA-PPyNP relative to PPyNP and HA also confirmed that HA was successfully incorporated in PPyNP (Fig. S2, ESI†).

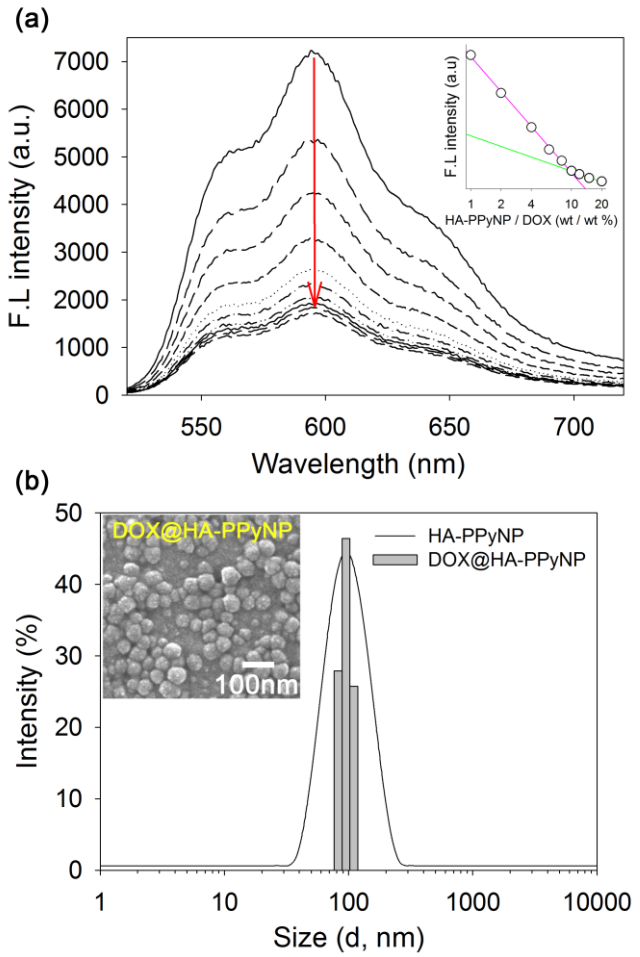

Fig. 2. (a) Fluorescence quenching of DOX after addition of various amounts of HA-PPyNP (from top to bottom: 0, 10, 20, 40, 60, 80, 100, 120, 150, 200 μg) (Inset: x-axis, HA-PPyNP to DOX ratio; y-axis, fluorescence intensity at 593 nm). (b) Hydrodynamic size distribution of HA-PPyNP and DOX@HA-PPyNP (Inset: SEM images of DOX@HA-PPyNP).

DOX-loaded HA-PPyNP (*i.e.*, DOX@HA-PPyNP) was prepared by forming a charge complex between positively charged DOX and the negatively charged HA layer of HA-PPyNP. We first determined whether the formation of the charge complex between DOX and HA-PPyNP resulted in fluorescence quenching of DOX. As mentioned above, PPyNP has immense absorption coefficients with a broad peak,[4] and therefore the fluorescence of DOX is expected to be quenched via fluorescence resonance energy transfer (FRET) from the excited DOX to PPyNP when they are located in close proximity. As expected, the fluorescence intensity of DOX was gradually reduced upon addition of an increasing amount of HA-PPyNP in the aqueous solution (Fig. 2a). In particular, we fitted two trend lines indicating log-linear decrease, suggesting that HA-PPyNP's quenching efficiency is not substantial after reaching a 1:10 ratio of DOX to HA-PPyNP (inset plot in Fig. 2a). Therefore, in the following experiments, DOX@HA-PPyNP was prepared at a 1:10 (wt/wt) mixing ratio.

When DOX@HA-PPyNP was prepared in a 1:10 ratio (that is, DOX:HA-PPyNP) and unbound free DOX was purified, the loading content of DOX in DOX@HA-PPyNP was determined to be 6.5% (wt/wt) from the analysis of UV/Vis absorption spectra. The mean hydrodynamic size of DOX@HA-PPyNP was similar (*i.e.*, 92.8 nm) with that of HA-PPyNP, but its size distribution was much narrower (Fig. 2b). The zeta potential of DOX@HA-PPyNP also increased to −21.4 mV compared with that of HA-PPyNP (−26.1 mV). These data support the negatively charged carboxyl groups in HA were partially neutralized by the charge interaction with the positively charged DOX. A relatively small increase in the zeta potential of DOX@HA-PPyNP compared with HA-PPyNP might indicate that DOX are located not on the outer part of the HA layer of HA-PPyNP but deep inside the HA layer, close to the PPyNP core. DOX@HA-PPyNP had a round-shaped morphology, as observed by scanning electron microscope (SEM) (Fig. 2b inset).

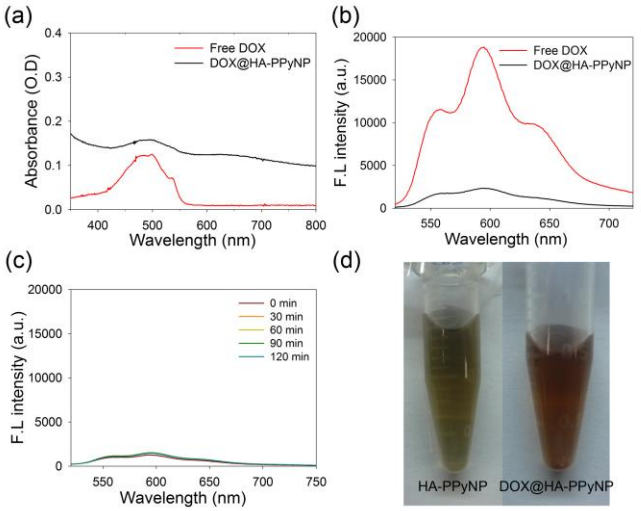

Fig. 3. (a) UV/Vis absorption and (b) fluorescence emission spectra of free DOX and DOX@HA-PPyNP (10 μM DOX equivalent). (c) Fluorescence intensity of DOX@HA-PPyNPs in the presence of serum proteins. (d) Dispersion stability of HA-PPyNP and DOX@HA-PPyNP in PBS solution containing 50% FBS. Pictures were taken after 1 week of incubation at room temperature.

Fig. 3a shows the UV/Vis absorption spectra of free DOX and DOX@HA-PPyNP at 10 μM DOX equivalent. The absorption spectrum of DOX loaded at HA-PPyNP became broader and weaker than that of free DOX at the same concentration (also see Fig. S4, ESI†). The fluorescence of DOX@HA-PPyNP was 8-fold lower than that of free DOX at the equivalent concentration (Fig. 3b). This quenching is believed to be induced by FRET from the DOX to PPyNP, but self-quenching between the DOX molecules, loaded onto the HA-PPyNP surface, might be possible.

Fluorescence quenching in DOX@HA-PPyNP was stably maintained in the presence of a high serum content (Fig. 3c). When we dispersed DOX@HA-PPyNP in phosphate buffer solution containing 50% (v/v) fetal bovine serum (FBS), there was only a 0.16× increase in the fluorescence of DOX during the 2 h incubation time, indicating that most of the DOX remained in the charge complex formation with HA and were not released into the solution. This can occur if DOXs are located in deeper positions of the HA layer of the particle surface as mentioned above, preventing an interaction between DOX and serum proteins. As shown in Fig. 3d,

no precipitate was observed for up to one week when both HA-PPyNP and DOX@HA-PPyNP were dispersed in the aqueous solution with a high serum content (50%), indicating excellent dispersion stability of these nanoparticles in the serum condition.

Next, we tested the drug-release behavior of DOX@HA-PPyNP at two different pH conditions (Fig. 4). At pH 7.4, only 54% of DOX was released from the nanoparticles over 48 h. In contrast, it took 8 h to obtain 57% drug release under acidic conditions (*i.e.*, pH 5.0), and the amount of the drug released reached approximately 100% after 24 h under this acidic pH condition. This can be explained if under acidic pH, the charge interaction between DOX and the carboxyl group was weakened due to the neutralization of carboxyl groups of HA, thereby stimulating drug release from DOX@HA-PPyNP. These data imply that the release of physically bound DOX molecules could be accelerated inside lysosomes of cells, while drug release in the neutral pH environment of the blood stream is significantly reduced.

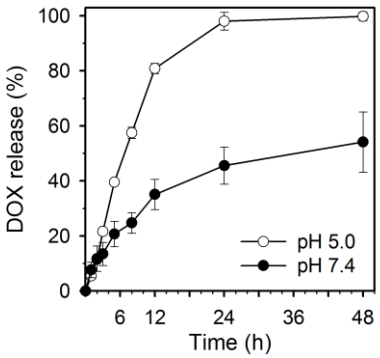

Fig. 4. pH-dependent drug release from DOX@HA-PPyNP (n = 3).

Next, the utility of DOX@HA-PPyNP in activatable fluorescence imaging of macrophage cells was tested in an *in vitro* live cell imaging study (Fig. 5a and S5, ESI†). Both free DOX and DOX@HA-PPyNP were applied to Raw264.7 macrophage cells at a concentration of 2 μM DOX equivalent. Since the fluorescence of DOX@HA-PPyNP is expected to be quenched in the extracellular environment and activated inside the acidic lysosomes of the macrophage cells because of stimulated drug release, the fluorescence images were obtained every 15 min for 3 h without washing the nanoparticles using a Live Cell Imaging System. As expected, only weak fluorescence signals were detected in the extracellular space of the DOX@HA-PPyNP-treated group for 3 h, and fluorescence intensities generated inside the cells became stronger over time, so the location of the macrophage cells could be clearly discriminated from the fluorescence images. When the cells were treated with free DOX, free DOX in the extracellular space was highly fluorescent and therefore it was hard to detect macrophage cells owing to the high background signals. These results support the potential utility of DOX@HA-PPyNP for the fluorescence imaging of atherosclerosis lesions with a high target-to-background ratio.

Before testing the *in vitro* therapeutic efficacy of DOX@HA-PPyNP, the cytotoxicity of HA-PPyNP was evaluated by treating macrophage cells with HA-PPyNP for 24 h over a concentration range of 0–500 μg/mL. Raw264.7 cells treated with HA-PPyNP showed no toxicity even at the highest concentration (Fig. S6, ESI†), implying that the nanoparticle itself is highly biocompatible and nontoxic to the macrophages. Then, the therapeutic potential of the pH-responsive DOX@HA-PPyNPs was tested (Fig. 5b). Raw264.7 cells were treated with DOX@HA-PPyNP for 3 h at various concentrations (0–5 μM DOX equivalent), washed three times to remove free drugs in the extracellular space, and further incubated for 48 h to allow proliferation of the macrophages. The viability of the cells was then evaluated. Human primary vascular smooth muscle cells (VSMCs) were used as a normal cell control, and treated with DOX@HA-PPyNP in the same conditions as the Raw264.7 cells above. About 60% of cell death of the proliferating macrophages was achieved at a concentration of 0.5 μM DOX equivalent, whereas more than 90% of VSMCs were viable in this condition. Cell viability of the macrophages dropped to 18.6% at a concentration of 2.5 μM DOX equivalent. However, 80% of VSMCs survived up to the concentration of 5 μM DOX equivalent.

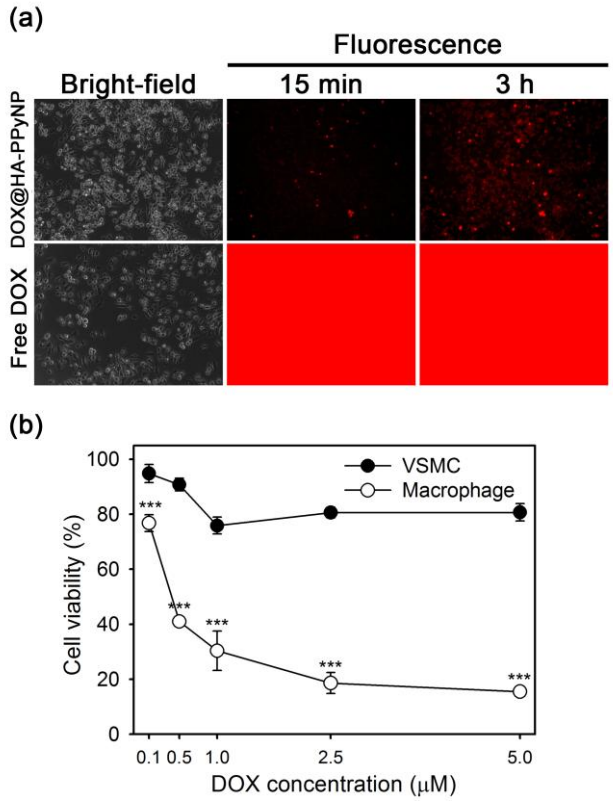

Fig. 5. (a) Live images of Raw 264.7 cells incubated with either free Dox or DOX@HA-PPyNP (2 μM DOX equivalent). Fluorescence images were obtained every 15 min for 3 h without washing the cells. Red color indicates fluorescence signals from DOX. (b) *In vitro* cytotoxicity of DOX@HA-PPyNP (n = 4). ***$P < 0.001$.

When VSMCs were treated with free DOX, significant cell death was observed for high concentrations of the drug, but the cell viability of DOX@HA-PPyNP-treated VSMCs was constant (Fig. S7a, ESI†). The cell viability of free DOX-treated macrophage cells was similar to that of DOX@HA-PPyNP-treated macrophages (Fig. S7b, ESI†). An additional cytotoxicity test and confocal microscopy study performed in the presence of free HA as a competitor supported the view that the therapeutic effect of DOX@HA-PPyNP on the proliferating macrophage cells was enhanced in part due to CD44-mediated endocytosis of the nanoparticles (see Fig. S8, ESI†).[10] CD44 expressed on the surface of activated macrophages is the principal receptor for HA. These *in vitro* cytotoxicity data indicate that DOX@HA-PPyNP might have great utility for the selective treatment of proliferating macrophages in atherosclerosis lesions while reducing the adverse side effect to normal cells.

In summary, DOX@HA-PpyNP showed high potential as a pH-responsive theranostic for imaging and therapy of proliferating macrophages in atherosclerosis lesions.

This work was supported by a National Cancer Center grant (1310160, 1410676 and 1410110), Republic of Korea.

Notes and references

[a] Molecular Imaging & Therapy Branch, National Cancer Center, 323 Ilsan-ro, Goyang-si, Gyeonggi-do 410-769, Korea. E-mail: ydchoi@ncc.re.kr; Fax: +82-31-920-2529; Tel: +82-31-920-2512
[b] New Experimental Therapeutics Branch, National Cancer Center, 323 Ilsan-ro, Goyang-si, Gyeonggi-do 410-769, Korea.
[c] Cancer Genomics Branch, National Cancer Center, 323 Ilsan-ro, Goyang-si, Gyeonggi-do 410-769, Korea. E-mail: andrea@ncc.re.kr; Fax: +82-31-920-2542; Tel: +82-31-920-2477.
† Electronic Supplementary Information (ESI) available: See DOI: 10.1039/c000000x/

1 World Health Organization, in *Global status report on noncommunicable diseases 2010*, ed. A. Alwan, WHO Press, Geneve, 2011, pp. 9-11.
2 (*a*) A. J. Lusis, *Nature*, 2000, **407**, 233.; (*b*) H. M. Wilson, R. N. Barker and L. P. Erwig, *Curr. Vasc. Pharmacol.*, 2009, **7**, 234.
3 M. Takeda, T. Yamashita, N. Sasaki, K. Nakajima, T. Kita, M. Shinohara, T. Ishida and K. Hirata, *Arterioscler. Thromb. Vasc. Biol.*, 2010, **30**, 2495.
4 (*a*) A. Yamaguchi, K. W. Woodburn, M. Hayase, G. Hoyt and R. C. Robbins, *Transplantation*, 2001, **71**, 1526.; (*b*) D. J. Kereiakes, A. M. Szyniszewski, D. Wahr, H. C. Herrmann, D. I. Simon , C. Rogers, P. Kramer, W. Shear, A. C. Yeung, K. A. Shunk, T. M. Chou, J. Popma, P. Fitzgerald, T. E. Carroll, D. Forer and Adelman DC, *Circulation*, 2003, **108**, 1310.
5 (*a*) Q. Liu and M. R. Hamblin, *Int. J. Immunopathol. Pharmacol,*. 2005, **1**8, 391.; (*b*) J. R. McCarthy, F. A. Jaffer and R. Weissleder, *Small*, 2006, **2**, 983.; (*c*) J. R. McCarthy, E. Korngold, R. Weissleder and F. A. Jaffer, *Small*, 2010, **6**, 2041.; (*d*) S. M. Shon, Y. Choi, J. Y. Kim, D. K. Lee, J. Y. Park, D. Schellingerhout and D. E. Kim, *Arterioscler. Thromb. Vasc. Biol.*, 2013, **33**, 1360.; (*e*) H. Kim, Y. Kim, I. H. Kim, K. Kim and Y. Choi, *Theranostics*, 2014, **4**, 1.
6 (*a*) V. Andrés, O. M. Pello and C. Silvestre-Roig, *Curr. Opin. Lipidol.*, 2012, **23**, 429.; (*b*) C. S. Robbins, I. Hilgendorf, G. F. Weber, I. Theurl, Y. Iwamoto, J. L. Figueiredo, R. Gorbatov, G. K. Sukhova, L. M. Gerhardt, D. Smyth, C. C. Zavitz, E. A. Shikatani, M. Parsons, N. van Rooijen, H. Y. Lin, M. Husain, P. Libby, M. Nahrendorf, R. Weissleder, F. K. Swirski, *Nat. Med.*, 2013, **19**, 1166.
7 E. R. Tavares, F. R. Freitas, J. Diament and R. C. Maranhão, *Int. J. Nanomedicine*, 2011, **6**, 2297.
8 (*a*) M. Chen, X. Fang, S. Tang and N. Zheng, *Chem. Commun.*, 2012, **48**, 8934.; (*b*) K. Yang, H. Xu, L. Cheng, C. Sun, J. Wang and Z. Liu, *Adv. Mater.*, 2012, **24**, 5586.
9 (*a*) J. C. Sluimer, F. D. Kolodgie, A. P. Bijnens, K. Maxfield, E. Pacheco, B. Kutys, H. Duimel, P. M. Frederik, V. W. van Hinsbergh, R. Virmani and M. J. Daemen, *J. Am. Coll. Cardiol.*, 2009, **53**, 1517.; (*b*) M. E. Lobatto, V. Fuster, Z. A. Fayad, W. J. Mulder, *Nat. Rev. Drug Discov.*, 2011, **10**, 835.
10 (*a*) M. Kamat, K. EI-Boubbou, D. C. Zhu, T. Lansdell, X. Lu, W. Li and X. Huang, *Bioconjug. Chem.*, 2010, **21**, 2128.